DOI: 10.1002/ejic.200600744

Tuning the Properties of Neutral Tetraazamacrocyclic Complexes of Copper(II) and Nickel(II) for Use as Host–Guest Compounds with Bismacrocyclic Transition Metal Cations

Anita Rybka,[a,b] Ryszard Koliński,[b] Jarosław Kowalski,[c] Rafał Szmigielski,[c] Sławomir Domagała,[d] Krzysztof Woźniak,*[d] Agnieszka Więckowska,[d] Renata Bilewicz,*[d] and Bohdan Korybut-Daszkiewicz*[a,c]

Keywords: Macrocyclic ligands / Copper / Nickel / Cyclic voltammetry / Template synthesis

The synthesis and structural properties of tetraazamacrocyclic ligands and their neutral and protonated 14-, 15- and 16-membered complexes of Cu^{II} and Ni^{II} are described. Molecules of the free 14-membered ligands have a nonplanar, step-like structure of the central molecular fragments. Conformational changes are introduced upon protonation, with the protons pointing above and below the macrocycle plane. This prevents the formation of intramolecular N–H···N hydrogen bonds. On insertion of the transition metal ions a planar structure of the macrocycle is obtained, which has consequences for the electrochemical behaviour of the complexes. The deviations from planarity increase with increasing macrocycle size. As a consequence the donor properties are weaker, the redox potential is shifted towards more positive values and the contribution of chemical reactions can be observed. The formation of host–guest complexes between the strongest metal-containing donors and transition-metal-containing bismacrocyclic acceptors of suitable size is proved in solution and the gas phase by voltammetric and ESI MS methods. The transition metal building blocks described in this contribution can be applied in the synthesis of new redox-active rotaxane and catenane systems.

Introduction

The well-known ability of azamacrocyclic ligands to stabilize unusual oxidation states of coordinated transition metal ions makes them a promising tool for the construction of molecular devices. Recently, we have reported the self-assembly of [2]catenanes built from an electron-rich component (dibenzo-24-crown-8) and an electron-deficient unsaturated bis-macrocyclic [14]cyclidene complex that coordinates two metal ions [either the same[1] or different (copper and nickel) [2]]. The electron-rich benzene rings of the interlocked crown ether in these compounds adopt a conformation that maximizes the donor–acceptor interactions with the bismacrocyclic subunit. By applying appropriate potentials, the coordinated metal ions can be oxidized selectively to the higher oxidation state (+3), which favours the interaction of these centres with the π-electron-rich aromatic rings of the crown unit. As a consequence, the relocation of the crown towards the oxidized metal centre takes place.

[a] Cardinal Stefan Wyszyński University, College of Science, Department of Mathematics & Natural Science, 01-815 Warszawa, Poland
[b] Institute of Physical Chemistry, Polish Academy of Sciences, Kasprzaka 44/52, 01-224 Warszawa, Poland
[c] Institute of Organic Chemistry Polish Academy of Sciences, Kasprzaka 44/52, 01-224 Warszawa, Poland
[d] Department of Chemistry, Warsaw University, Pasteura 1, 02-093 Warszawa, Poland
Fax: +48-22-8222892
E-mail: kwozniak@chem.uw.edu.pl

The introduction of an additional transition metal centre into similar supramolecular systems would enhance the prospects for the control of their properties. Therefore, the aim of this work is to synthesise some neutral macrocyclic complexes of the transition metals which could be used as π-electron-rich building blocks for the self-assembly of intertwined molecules. We have focused on dianionic tetraimine macrocyclic ligands substituted in the *meso* positions with some reactive groups. These groups could then be used for the extension of the ligand superstructure. The synthesis of the 14-membered tetraimine **4** (see Scheme 1) was recently reported by Takamura,[3a] although the 15- (**5**) and 16-membered (**6**) analogues were not accessible by this procedure. We have synthesised the 15- and 16-membered derivatives following a template Jäger synthetic strategy[4,5] from 2-formyl-3-hydroxypropenoic methyl ester and the appropriate diamines.

In this paper, we describe the synthesis of a series of neutral azamacrocyclic complexes of Cu and Ni and characterise their structures and redox properties. We also demonstrate their unique complexing abilities, which can be tuned simply by changing the size of the macrocycles in the host and guest molecules. The latter property is of special importance since the macrocyclic complexes may be considered as building blocks for new rotaxane-like meccano-molecular devices, which are one of the long-term goals of our project.

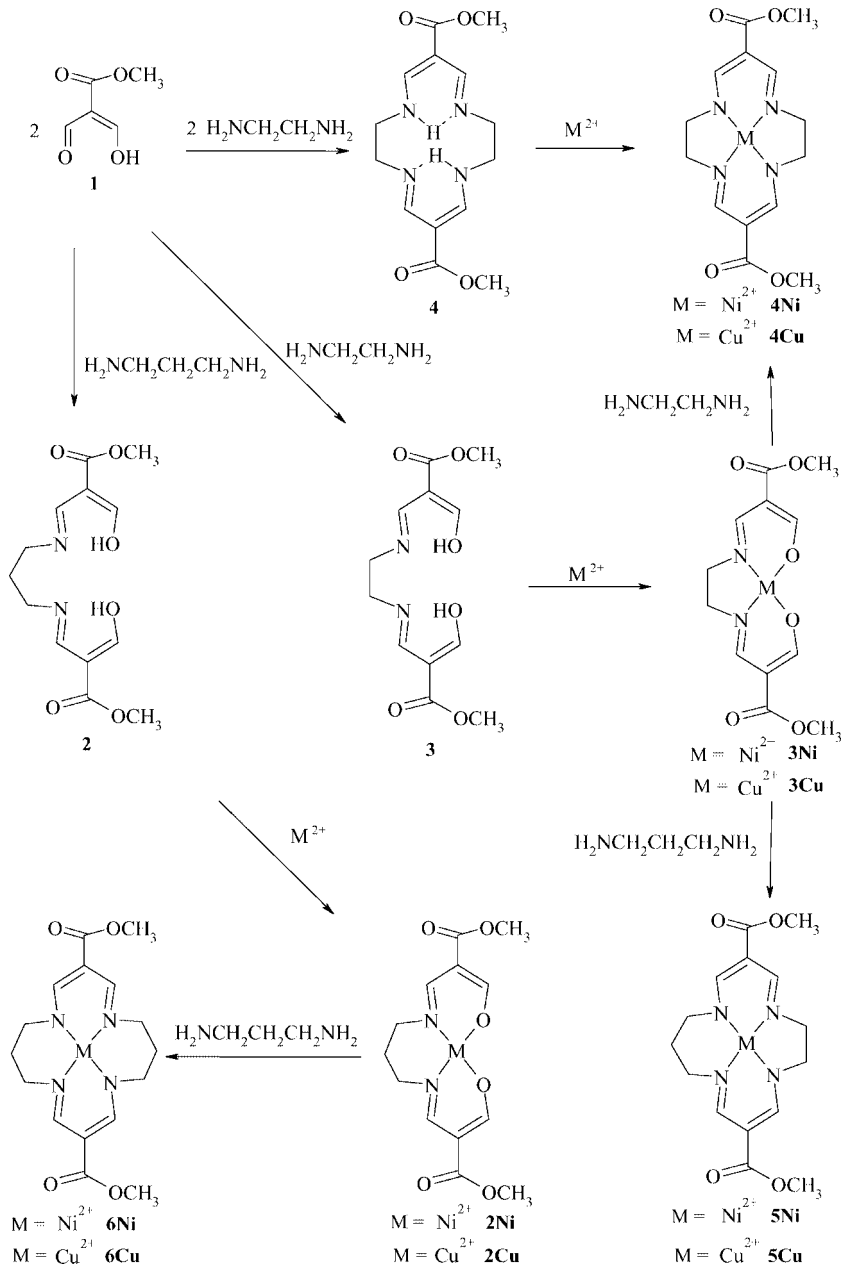

Scheme 1. Synthesis of neutral macrocyclic complexes of Ni^{II} and Cu^{II}.

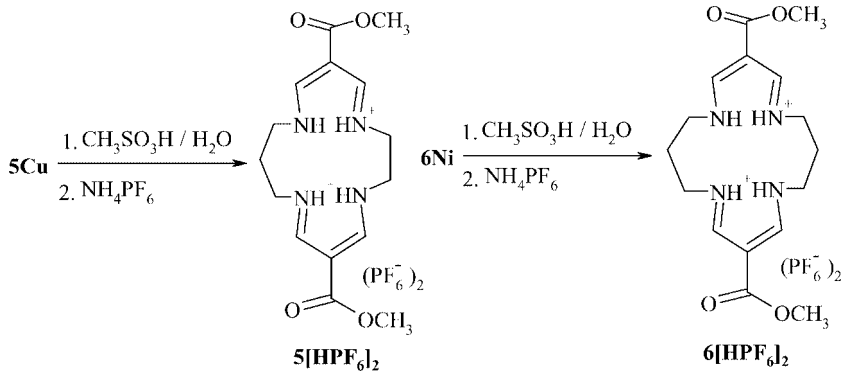

Scheme 2. Demetallation of complexes **5Cu** and **6Ni**.

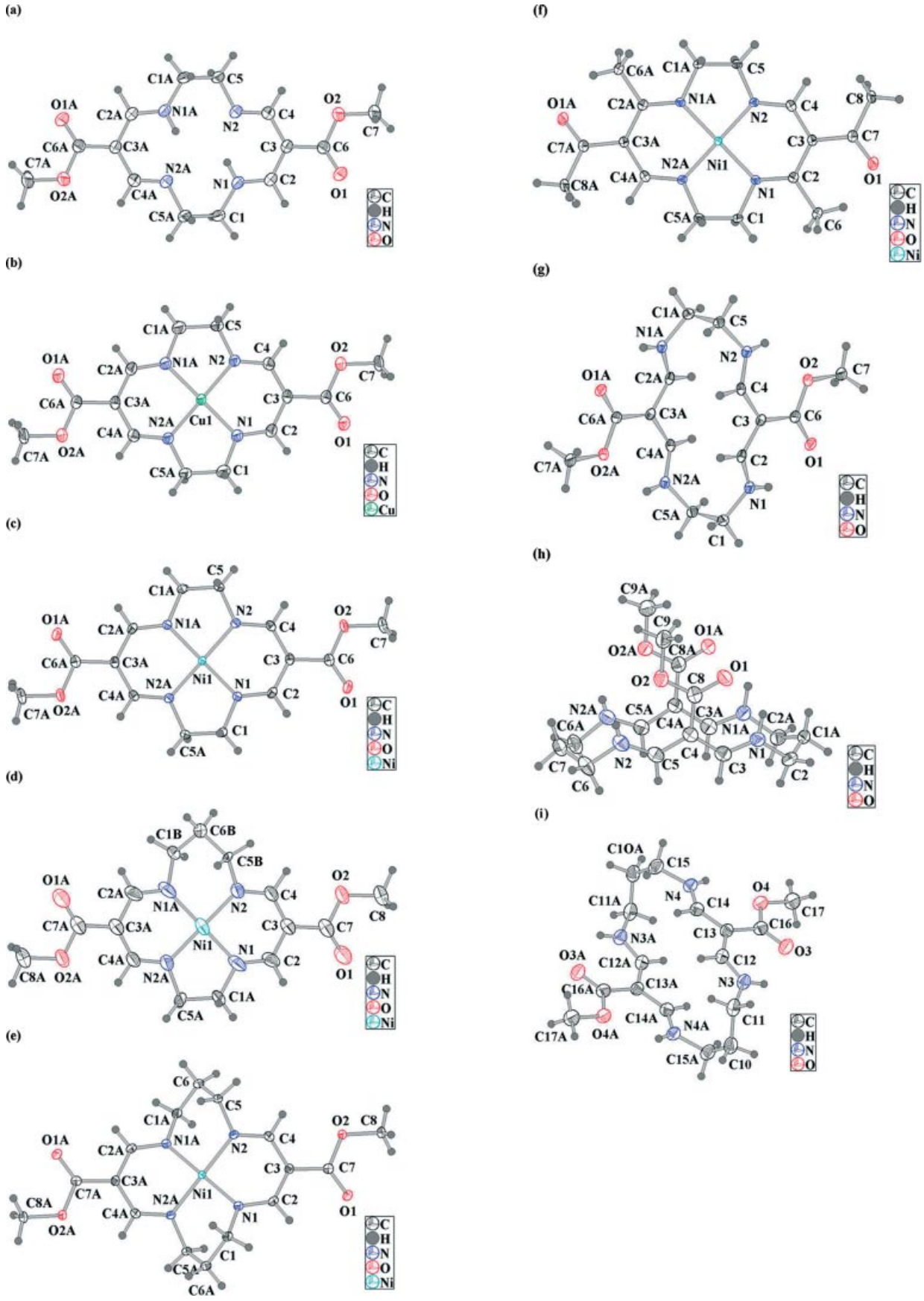

Figure 1. Thermal ellipsoids and atom numbering schemes in **4** (a), **4Cu** (b), **4Ni** (c), **5Ni** (d), **6Ni** (e), **10Ni** (f), **4[HCl]$_2$** (g) and the first (h) and second (i) molecules of **6[HPF$_6$]$_2$**. The atoms related by symmetry are labelled with the letter "A".

Results and Discussion

Synthesis

The synthesis of the nickel(II) and copper(II) complexes **4Ni**, **4Cu**, **5Ni**, **5Cu**, **6Ni** and **6Cu** is summarised in Scheme 1. The 14-membered ligand **4** was obtained by direct condensation of an equimolar mixture of 2-formyl-3-hydroxypropenoic methyl ester[3b] and ethylenediamine.[3a] Refluxing the ligand **4** with nickel(II) or copper(II) acetate in methanol solution gave the neutral complexes **4Ni** and **4Cu**, respectively. The reaction of 2-formyl-3-hydroxypropenoic methyl ester with diamines in a 2:1 ratio followed by complexation with nickel or copper acetate gave the complexes **2Ni** or **3Ni** and **2Cu** or **3Cu**, respectively.[6] The template reaction with a second diamine molecule afforded the 15- and 16-membered complexes. However, the reaction of the chelates **2Ni** and **2Cu** with an excess of ethylenediamine produced mainly the 14-membered complexes **4Ni** and **4Cu**, respectively.

The decomplexation of **5Cu** and **6Ni** by treatment with an excess of methanesulfonic acid in aqueous solution, followed by precipitation with NH_4PF_6, afforded the free ligands as their diprotonated hexafluorophosphates **5[HPF$_6$]$_2$** and **6[HPF$_6$]$_2$**, respectively (Scheme 2).

Structural Properties

Figure 1 shows thermal ellipsoid representation of atoms with atomic labels for the series of neutral and protonated macrocyclic compounds studied and their complexes with Ni^{II} or Cu^{II} ions. All compounds crystallise in centrosymmetric space groups with molecules located at special positions (inversion centre or mirror plane). Therefore, only half of all atoms constituting a given molecule and corresponding solvent molecules, or counterions, are independent in all cases (see the Experimental Section for crystallographic details).

All the compounds described are composed of tetraazamacrocyclic rings with different numbers of atoms (14, 15 or 16). The electron density of the 16-membered rings is delocalised over the chelate rings and the functional groups. As a result, a bond-length alternation is present in those parts of the molecules. In the case of **4Cu**, **4Ni**, **5Ni**, **6Ni** and **10Ni**[4,5,7] the Cu^{II} or Ni^{II} ions are coordinated by the nitrogen atoms from the macrocyclic ligands to form square-planar complexes. In the free ligands (**4[HCl]$_2$** and **6[HPF$_6$]$_2$**), all of the nitrogen atoms are protonated and the conformation of the molecule is completely different. In all cases, except for **10Ni**, the macrocyclic ring is functionalised with two methoxycarbonyl groups, which can adopt either *trans* or *cis* conformations (see Figure 1, parts h and i). The 14-membered ring of **10Ni** has two types of substituents, namely two acyl and two methyl groups located *trans* to each other, thus confirming the structural results of Alcock et al.[7] and contrary to earlier reports.[4,5] The 14-membered macrocyclic ring in the structure of the free ligand **4** is not coplanar. Due to the coordination of Cu and Ni by the nitrogen atoms of the ring, the structures of the complexes formed (**4Cu**, **4Ni**, **5Ni**, **6Ni** and **10Ni**) are more planar than those of the free ligands. The RMS deviation of the fitted atoms to the least-square plane L^1 varies from 0.04 to 0.09 Å for the 14-membered complexes, whereas for the free ligands it is equal to 0.23 Å. Some smaller values of the angles between the previously defined plane and the plane fitted to the atoms of the ethylene bridges L^2 for Ni and Cu complexes indicate the more planar nature of the complexes (see Table 1 and Figure 2).

Table 1. Values of the RMS deviation [Å] of all the fitted atoms and angles [°] between the least-squares planes L^1 and L^2. L^1 is defined by the following sequence of atoms: M1, N1, N2, C2, C3, C4, N1#1, N2#1, C2#1, C3#1, C4#1, where M is a metal ion, and L^2 is based on the ethylene or propylene (**5Ni** and **6Ni**) groups: C1, C5, C1#1, C5#1 or C1A C5A, C1B, C5B and C6B for **5Ni**.[a]

Least-squares plane	**4**	**4Cu**	**4Ni**	**10Ni**	**5Ni**	**6Ni**
L^1	0.2291	0.0400	0.0696	0.0910	0.1413	0.2189
L^1–L^2 angle	36.4(1)	22.4(2)	26.9(1)	26.6(1)	41.4(3)	46.65(4)

[a] Symmetry transformations used to generate equivalent atoms: #1 1 – *x*, 1 – *y*, 1 – *z*.

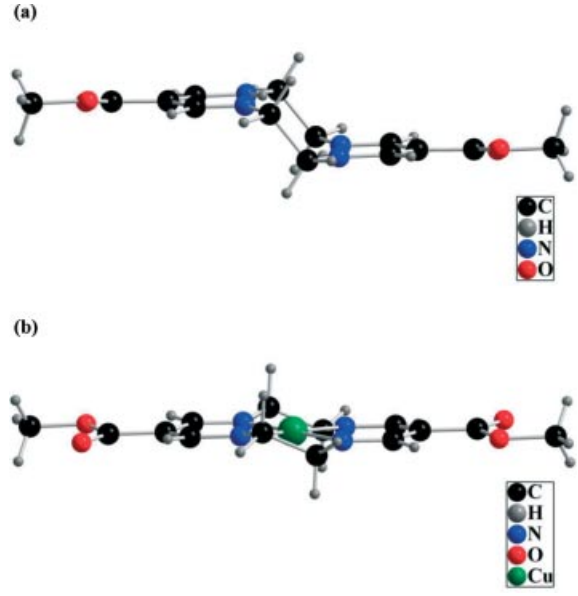

Figure 2. The structure of **4** (a) and **4Cu** (b).

The Ni–N and Cu–N distances vary within the ranges 1.836–1.890 and 1.912–1.922 Å and are typical for Ni and Cu complexes (see Table 2). The Ni–N distance increases with increasing size of the main macrocyclic ring (**4Ni**, **5Ni**, **6Ni**).

The compounds **4[HCl]$_2$** and **6[HPF$_6$]$_2$** have totally different structures. As a result of demetallation of the corresponding complexes, both imine nitrogen atoms in these compounds are protonated to form ammonium groups. Due to some steric hindrance coming from the interactions between the closely located hydrogen atoms, a change of the

Table 2. Selected bond lengths and distances [Å]. L^1: least-squares plane defined by the following sequence of atoms: M1, N1, N2, C2, C3, C4, N1#1, N2#1, C2#1, C3#1, C4#1, where M is a metal ion; X_1: centroid of the N1, N2, N1#1 and N2#1 atoms.

Parameter[a]	**4Ni**	**4Cu**	**4**	**10Ni**	**5Ni**	**6Ni**	**4**$[HCl]_2$	**6**$[HPF_6]_2$[b]
M1···M1#2	6.3188(5)	6.322(1)		4.7792(4)	6.714(1)	7.6007(5)		
L^1···M1#2	3.303(1)	3.333(3)		3.617(2)	3.287(5)	3.062(2)		
L^1···X_1#2			4.269					
M1–N1	1.856(1)	1.912(2)		1.882(1)	1.871(4)	1.892(1)		
M1–N2	1.851(1)	1.922(2)		1.836(1)	1.865(3)	1.890(1)		
O1–C6	1.216(2)	1.213(3)	1.220(3)				1.228(2)	
O1–C7				1.244(2)	1.199(5)	1.221(2)		
O1–C8								1.207(5)
O2–C6	1.363(2)	1.360(3)	1.362(3)				1.346(2)	
O2–C7	1.439(2)	1.446(3)	1.443(3)		1.357(5)	1.365(2)	1.460(2)	
O2–C8					1.443(5)	1.444(2)		1.339(4)
N1–C1	1.474(2)	1.473(4)	1.450(3)	1.482(2)		1.481(2)	1.469(2)	
N1–C1A					1.449(9)			
N1–C1B#1					1.556(9)			
N1–C2	1.306(2)	1.308(3)	1.316(3)	1.316(2)	1.304(6)	1.310(2)	1.317(2)	1.476(5)
N1–C3								1.302(5)
N2–C4	1.307(2)	1.300(3)	1.288(3)	1.303(2)	1.295(5)	1.309(2)	1.310(2)	
N2–C5	1.473(2)	1.480(3)	1.463(3)	1.464(2)		1.473(2)	1.475(2)	1.295(5)
N2–C5A#1					1.47(1)			
N2–C5B					1.54(1)			
C1–C5#1	1.518(2)	1.506(5)	1.527(3)	1.511(2)			1.540(2)	
C1A–C5A					1.50(2)			
C1–C6#1						1.533(2)		
C1B–C6B					1.54(1)			
C5–C6						1.521(2)		
C5B–C6B					1.55(1)			
C2–C3	1.408(2)	1.417(4)	1.395(3)	1.448(2)	1.410(6)	1.415(2)	1.412(2)	
C2–C6				1.512(2)				
C3–C4	1.413(2)	1.412(4)	1.442(3)	1.411(2)	1.404(6)	1.406(2)	1.420(2)	1.411(5)
C3–C6	1.456(2)	1.465(4)	1.451(3)				1.471(2)	
C3–C7				1.453(2)	1.461(6)	1.453(2)		

[a] Symmetry transformations: #1: 1 – *x*, 1 – *y*, 1 – *z*; #2: 1 + *x*, *y*, *z* (**4Ni**, **5Ni**, **6Ni**, **10Ni**); *x*, 1 + *y*, *z* (**4Cu**). [b] Additionally for **6**$[HPF_6]_2$: O2–C9 1.442(5), O3–C16 1.212(5), O4–C16 1.332(4), O4–C17 1.459(4), N2–C6 1.464(5), N3–C11 1.468(5), N3–C12 1.312(5), N4–C14 1.300(5), N4–C15 1.482(5), C1–C2 1.517(5), C4–C5 1.405(5), C4–C8 1.467(5), C6–C7 1.516(5), C10–C11 1.509(6), C10–C15#3 1.511(6), C12–C13 1.389(5), C13–C14 1.395(5), C13–C16 1.480(5) Å (#3: 1/2 – *x*, 1/2 – *y*, 1/2 – *z*).

Table 3. Geometry of the hydrogen bonds [Å and °] in the compounds studied.

D–H···A	Symmetry	*d*(D–H)	*d*(H···A)	*d*(D···A)	<(DHA)
4					
N1–H1N···N2	*x*, *y*, *z*	0.88(3)	1.93(3)	2.656(3)	138(2)
10Ni					
O1W–H1W1···O1	*x*, *y*, *z*	0.77(2)	2.06(2)	2.826(2)	172(2)
O1W–H2W1···O1W	–*x*, –*y*, –*z*	0.69(4)	2.13(4)	2.815(3)	172(5)
O1W–H3W1···O1W	1 – *x*, –*y*, –*z*	0.76(4)	2.07(4)	2.810(3)	163(4)
4$[HCl]_2$					
N1–H1N···O1	*x*, *y*, *z*	0.82(2)	2.12(2)	2.731(2)	131(1)
N2–H2N···O2	*x*, *y*, *z*	0.89(2)	2.14(2)	2.719(2)	122(1)
N2–H2N···O1W	*x*, *y*, *z*	0.89(2)	2.04(2)	2.823(2)	147(1)
O1W–H1W···Cl1	1 + *x*, *y*, *z*	0.82(2)	2.36(2)	3.177(2)	176(2)
O1W–H2W···Cl1	1 – *x*, 2 – *y*, 1 – *z*	0.87(3)	2.30(3)	3.168(2)	177(2)
6$[HPF_6]_2$					
N1–H1N···O1	*x*, *y*, *z*	0.96(4)	1.99(4)	2.678(4)	127(3)
N2–H2N···O2	*x*, *y*, *z*	0.68(4)	2.31(4)	2.738(5)	123(4)
N3–H3N···O3	*x*, *y*, *z*	0.88(4)	2.14(4)	2.751(4)	127(3)
N4–H4N···O4	*x*, *y*, *z*	0.80(5)	2.25(5)	2.781(4)	125(4)
N1–H1N···F11	*x*, *y*, *z*	0.96(4)	2.49(4)	3.088(5)	120(3)
N2–H2N···F15A	1 – *y*, *x*, *z*	0.68(4)	2.50(4)	3.140(7)	158(4)
N3–H3N···F8	*x*, *y*, *z*	0.88(4)	2.48(4)	3.042(4)	122(3)
N4–H4N···F6	*y*, –*x*, *z*	0.80(5)	2.32(5)	3.013(4)	145(4)

conformation of the whole moiety takes place. The CHNH groups are rotated about the C–N bond, thus the N–H bonds are oriented outside of the ring whereas the C–H bonds are directed inside. Therefore, the distance between the ethylene bridges is elongated whereas the separation between the methoxycarbonyl groups decreases. Such a conformation is stabilized by numerous intramolecular hydrogen bonds formed between the nitrogen and oxygen atoms from the ester groups (see Table 3 and Figure 3).

In neutral compounds, hydrogen bonds are formed between the macrocycles and some solvent molecules (**10Ni**) or between the nitrogen atoms in the main macrocyclic ring (**4**).

The crystal packing of the compounds is shown in Figure 4. The molecules of the neutral compounds create parallel and slightly shifted stacks in the crystal lattice. The distances between the neighbouring macrocyclic rings in the crystal lattice vary from 3.062 to 3.617 Å and are given in Table 2.

In the structures of **4Ni** and **5Ni**, disordered solvent (toluene) molecules are located at special positions and form layers of molecules sandwiched between layers of the macrocyclic moieties. The toluene molecules are oriented so as to maximize the C–H···π interaction between the electron-rich benzene rings and the hydrogen atoms from the ethylene bridges. These compounds crystallise in the $P\bar{1}$ space group, whereas the protonated compounds crystallise in different space groups. The voids between neighbouring molecules in the structures are filled with counterions in the case of protonated ligand salts or solvent molecules.

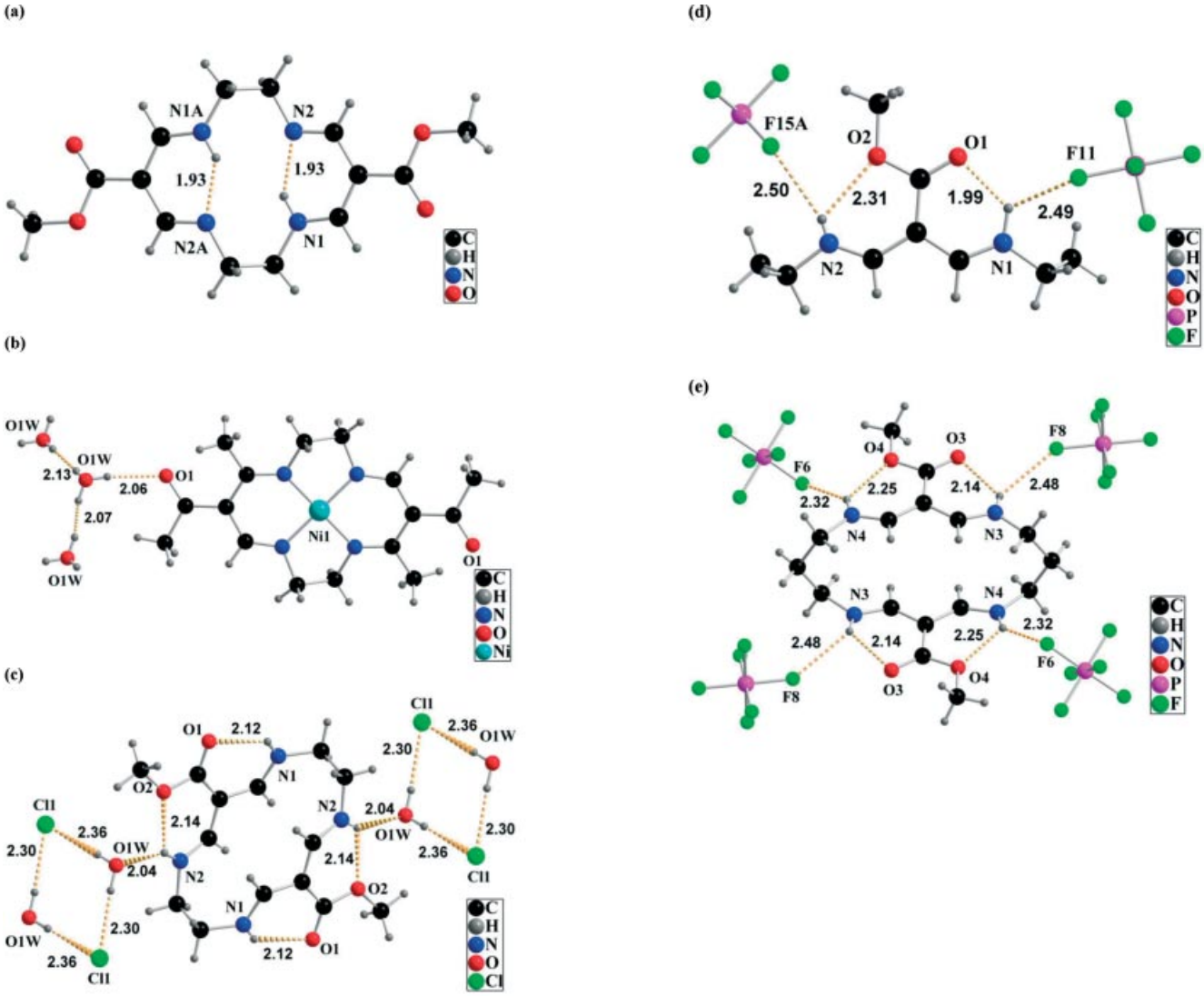

Figure 3. Hydrogen bonds formed by molecules of **4** (a), **10Ni** (b), **4[HCl]$_2$** (c) and the first (d) and second (e) molecules of **6[HPF$_6$]$_2$**.

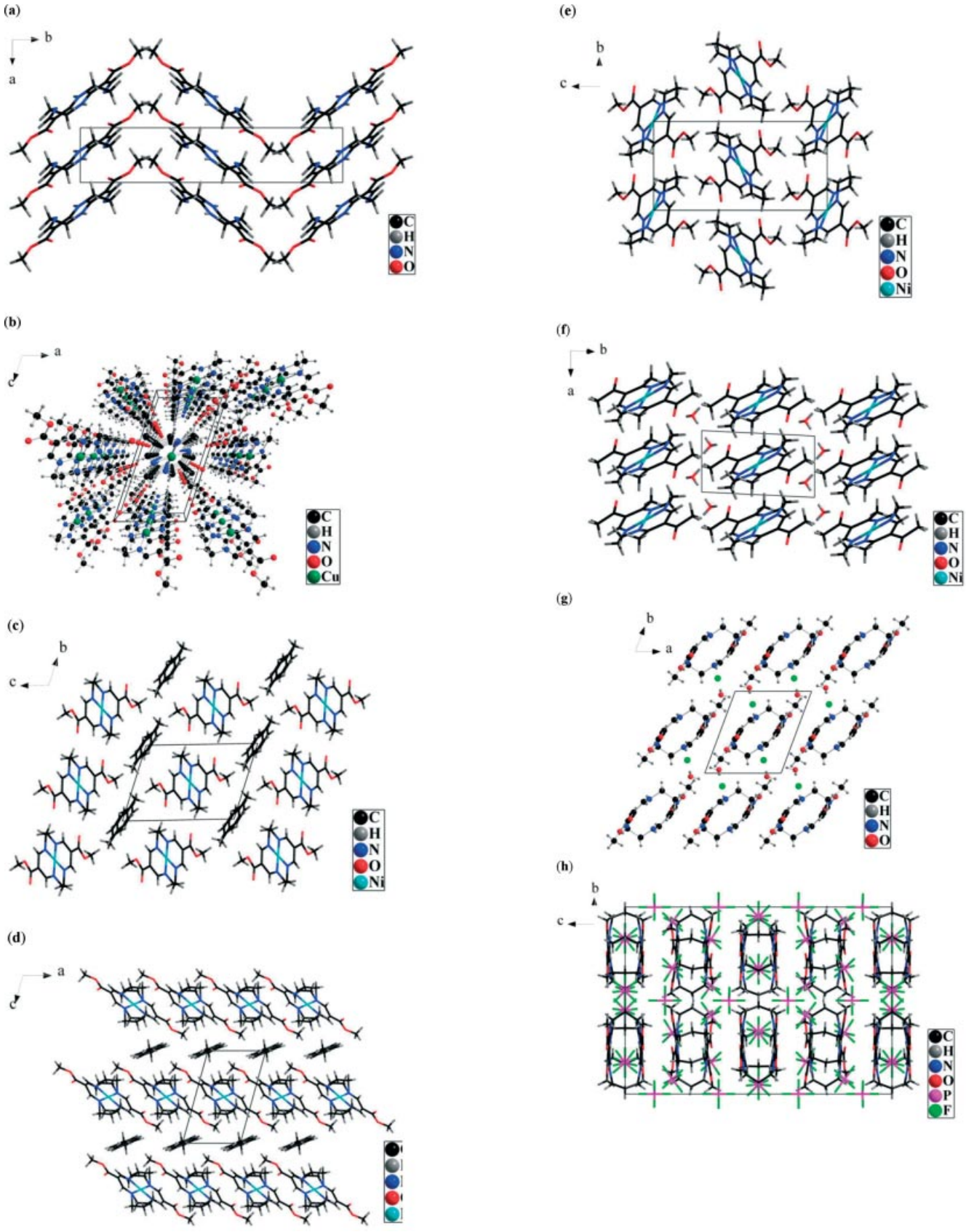

Figure 4. Selected perspective views of the crystal packing in **4** (a), **4Cu** (b), **4Ni** (c), **5Ni** (d), **6Ni** (e), **10Ni** (f), **4[HCl]$_2$** (g) and **6[HPF$_6$]$_2$** (h).

Voltammetry

The linear-scan, differential and normal-pulse voltammograms recorded for **4Cu**, **5Cu** and **6Cu** indicate a striking difference in the formal potentials with no major deviations from reversibility (see Figure 5). Upon increasing the macrocycle size, the donor abilities of the Cu^{II} complex become weaker — the mid-potential $(E_{p_c} + E_{p_a})/2$ is shifted towards more positive potentials by as much as 330 mV. The peak current is also smaller, although the complex is soluble in the supporting electrolyte solution. This shift is not seen for the corresponding Ni^{II} complexes (Figure 6) and reveals that the smaller ring in **4Cu** has a more planar coordination environment of the copper centre, which allows reversible oxidation to the Cu^{III} complex. We have noted a similar dependence on the macrocycle size for other tetraazamacrocyclic complexes of copper.[8] In these compounds a decrease of the Cu^{III} reduction current was observed together with a shift to more positive potentials. This indicates that the electron-transfer reaction is followed by a chemical reaction.

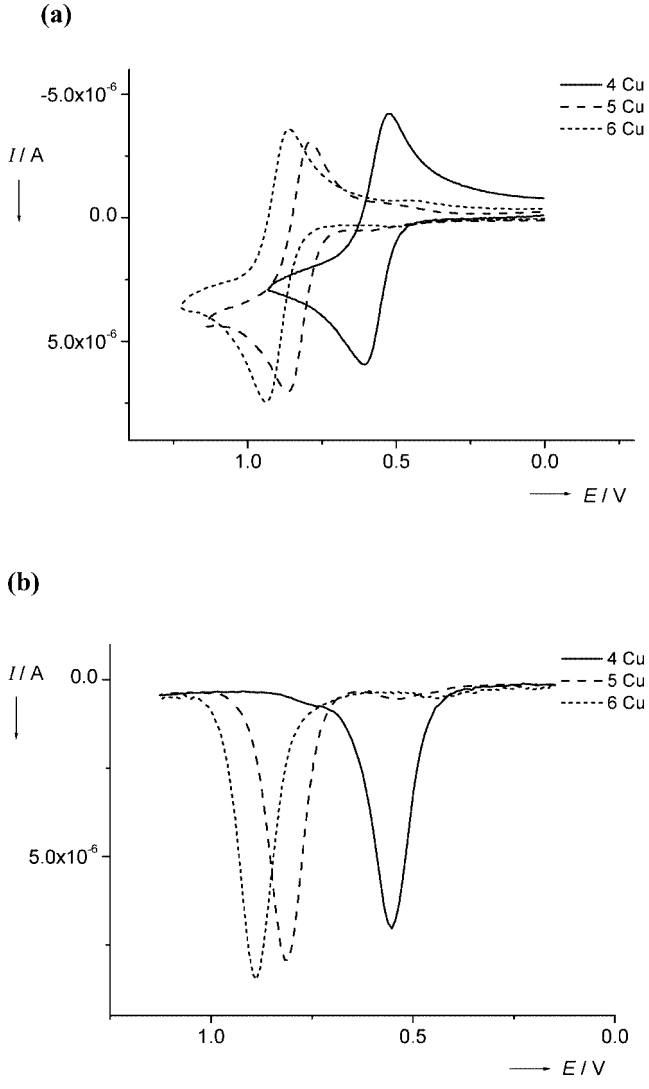

Figure 5. Cyclic voltammograms (a) and differential pulse voltammograms (b) for 0.5 mM **4Cu**, **5Cu** and **6Cu** complexes recorded using a GCE in 0.1 M tetrabutylammonium hexafluorophosphate (TBAHFP)/acetonitrile (AN) solution.

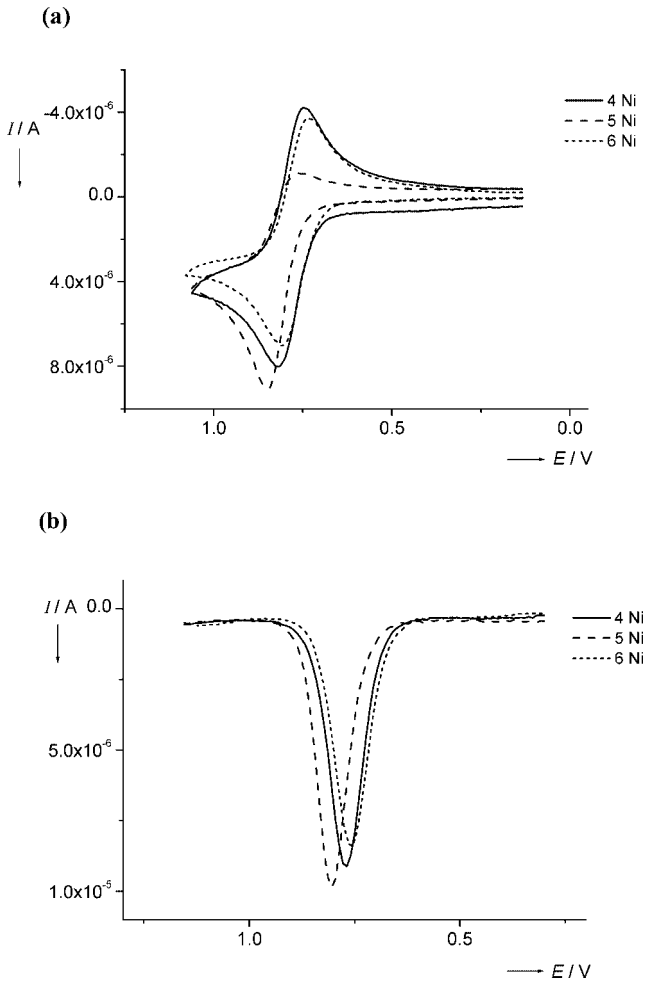

Figure 6. Cyclic voltammograms (a) and differential pulse voltammograms (b) for 0.5 mM **4Ni**, **5Ni** and **6Ni** recorded using a GCE in 0.1 M TBAHFP/AN solution.

In the compounds presented in this contribution, the electrode processes of all copper complexes clearly remain close to reversible and no chemical reactions are involved. The changes in the redox potential with increasing macrocycle size can be explained by assuming increased non-planarity of the complex. The structures of the larger systems[7,8] show deviations from planarity. On the other hand, in the case of **5Ni** a diminished cathodic peak reveals an instability of Ni^{III} and involvement of further chemical reactions. The redox properties and diffusion coefficient values, based on the voltammetry peaks or limiting currents, are collected in Table 4.

Table 4. Redox properties and diffusion coefficients of the Cu^{II} and Ni^{II} complexes studied.

	CV			DPV	NPV	D
	E_{pa} [V]	E_{pc} [V]	$E^{o\prime}$ [V]	E_p [V]	$E_{1/2}$ [V]	10^{-5} [$cm^2 s^{-1}$]
4Ni	0.817	0.749	0.783	0.768	0.783	1.15
5Ni	0.852	0.759	0.806	0.804	0.819	1.72
6Ni	0.811	0.738	0.775	0.755	0.769	1.02
4Cu	0.605	0.527	0.566	0.552	0.565	0.70
5Cu	0.862	0.788	0.825	0.809	0.827	0.95
6Cu	0.940	0.862	0.901	0.887	0.989	1.12

Host–Guest Interactions

The bis-macrocyclic receptors shown in Scheme 3[9,10] have been shown to form host–guest complexes with π-electron-rich aromatic guests.[11] Their structures are based on donor–acceptor interactions between the π-electron-rich aromatic rings and π-electron-deficient cyclidene units. The same type of interactions should result in the affinity of such receptors towards the planar, neutral complexes **4Cu** and **4Ni**.

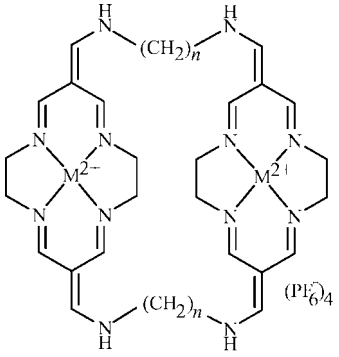

$n = 5$, M = Ni **7NiNi**
$n = 7$, M = Ni **8NiNi**
$n = 7$, M = Cu **8CuCu**
$n = 9$, M = Ni **9NiNi**
$n = 9$, M = Cu **9CuCu**

Scheme 3. Structures of the host complexes.

The changes of the cyclic voltammogram for **4Cu** alone, and after mixing with bis-macrocyclic receptor **8NiNi**, are shown in Figure 7. The midpoint potential $E^{o\prime} = (E_{pa} + E_{pc})/2$ is shifted by 20 mV towards less positive potentials upon mixing with the excess of bis-macrocycle, thereby indicating the stronger donor properties of the complex. These stronger donor properties may be interpreted as an indication of the associative properties of the bis-macrocyclic complex towards the **4Cu** moiety. Thus, **8NiNi** may be acting as a receptor molecule towards the guest planar **4Cu** complex. These unique complexing properties were probed by electrospray mass spectrometry (ESI-MS).

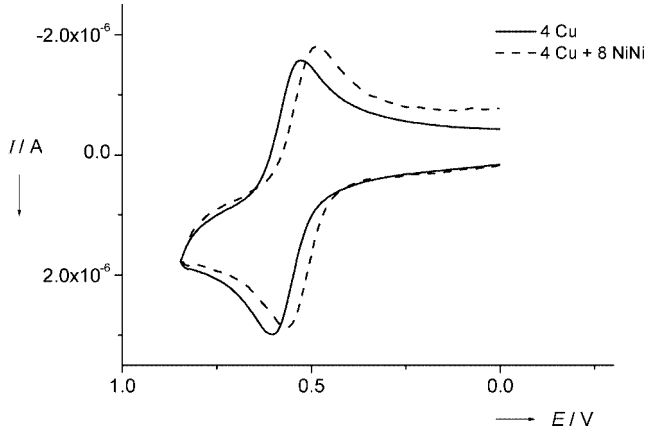

Figure 7. Cyclic voltammograms for 1×10^{-4} M **4Cu** and its 1:10 mixture with **8NiNi** after 5 d. Scan rate: 0.1 $V s^{-1}$. GCE in 0.1 M TBAHFP/AN solution.

Despite the fact that ESI-MS might not reflect the solution binding affinities accurately, it provides important information on host–guest complexes and the nature of their interactions.[12] The ESI mass spectra of an equimolar mixture (10^{-3} M) of neutral complexes **4Cu** or **4Ni** and bis-macrocyclic receptors **8NiNi** or **8CuCu** in dichloromethane/acetonitrile (1:3) solution confirmed the formation of the host–guest complexes. New peaks at *m*/*z* 437.2, 438.9, 440.5, 442.2 corresponding to the formation of the 1:1 adducts **8NiNi+4Ni**, **8NiNi+4Cu**, **8CuCu+4Ni** and **8CuCu+4Cu**, respectively, with a +4 charge, were observed in the spectra of their mixtures. In order to compare the affinities of bis-macrocyclic receptors towards neutral guests, the ESI mass spectra of equimolar mixtures of **7NiNi**, **8NiNi** and **9NiNi** with **4Cu** were measured (Figure 8, a). The spectra show that the cavity size in **7NiNi**, which contains $(CH_2)_5$ linkers, is too small to accommodate the guest molecules and no common peaks were recorded. On the other hand, the cavity size in **9NiNi**, which contains $(CH_2)_9$ linkers, is too large to enable simultaneous and equally strong interactions of guest molecules with both sides of the receptor cation, therefore the intensity of the common peak (*m*/*z* 457.5) is very low in comparison with the peak of the **8NiNi+4Cu** associate (*m*/*z* 438.9). A comparison of the dinickel (**8NiNi**) and dicopper (**8CuCu**) receptors (Figure 8, b) shows their similar affinities towards the **4Cu** guest. On the other hand, the neutral **4Cu** complex forms a more stable associate with **8NiNi** than its nickel(II) analogue **4Ni** (see Figure 8, c).

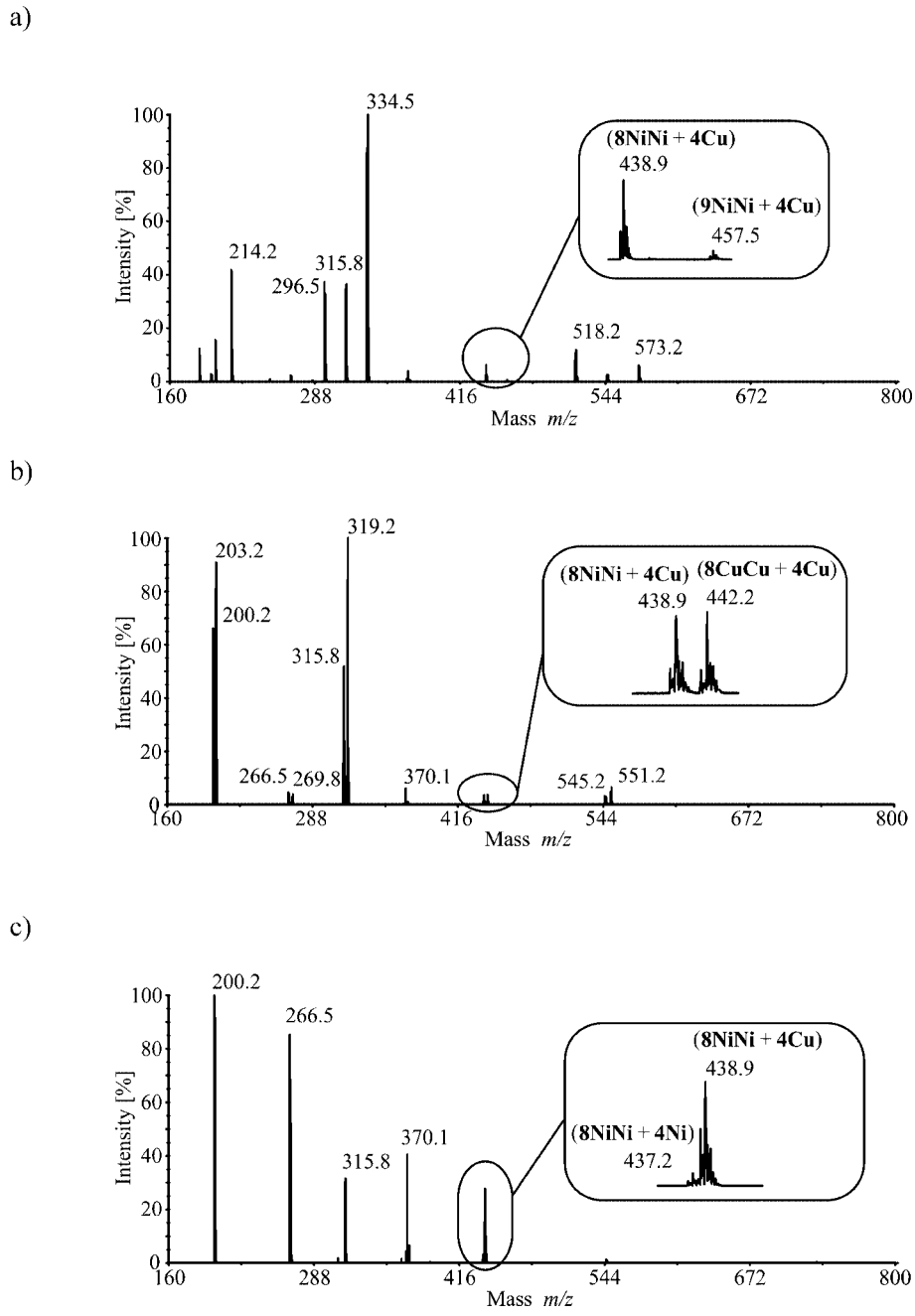

Figure 8. ESI mass spectra of equimolar mixtures of **7NiNi**, **8NiNi** and **9NiNi** with **4Cu** (a), **8NiNi** and **8CuCu** with **4Cu** (b) and (c) **4Ni** and **4Cu** with **8NiNi**.

Conclusions

In this work we have presented the synthesis and structural properties of ligands and their neutral 14-, 15- and 16-membered complexes with Cu^{II} and Ni^{II}. It appears that molecules of the free 14-membered ligands have a non-planar, step-like structure of the ethylene bridges. Significant changes in the geometry of the central macrocyclic fragments are observed on protonation as the protons no longer occupy the central positions of the ring but point above and below the macrocycle plane. This prevents the formation of intramolecular N–H···N hydrogen bonds. The insertion of transition metal ions is accompanied by an increased planarity of the structures of the complexes, which has consequences for the electrochemical reversibility and redox potentials of the complexes. The deviations from planarity increase with increasing macrocycle size and, as a consequence, the redox potential is shifted towards more positive values. In the case of the Ni^{II} complexes, a contribution of chemical reactions is detected by the decrease of the reduction peak.

The formation of host–guest complexes with bis-macrocyclic cations can be achieved by appropriate tuning of the properties of the macrocyclic complexes, as demonstrated for planar, neutral macrocyclic guests associating with the bis-macrocyclic **8NiNi** (or **8CuCu**) cation receptors. This type of interaction, which leads to a new transition-ion complex structure, is of special interest in the design of new rotaxane-like systems for mechano-molecular devices, and work in this direction is currently underway in our laboratories.

Experimental Section

Synthesis: 6,13-Bis(methoxycarbonyl)-1,4,8,11-tetraazacyclotetradeca-4,6,11,13-tetraene (**4**),[3] ligands **2** and **3** as well as their nickel(II) [(**2Ni**)$_2$·Ni(CH$_3$COO)$_2$·2CH$_3$OH and **3Ni**] and copper(II) complexes (**2Cu** and **3Cu**)[6] were obtained according to procedures described elsewhere. Crystals of the neutral nickel(II) complex **10Ni**[4,5] were obtained by slow evaporation of its solution in a 1:1 dichloromethane/methanol mixture.

Spectroscopic Measurements: The NMR spectra were obtained with Varian Mercury 400 and Varian Gemini 2000BB spectrometers. Signals are reported in ppm relative to the residual solvent signal. IR spectra (paraffin oil mulls) were recorded with a Perkin–Elmer Spectrum 2000 FT-IR spectrometer. UV/Vis absorption spectra were recorded with a Shimadzu UV-3100 spectrometer. ESI mass spectra were measured with a Mariner Perseptive Biosystem mass spectrometer.

Voltametry: Linear-scan, differential-pulse and normal-pulse voltammetry experiments were performed with an Autolab potentiostat (ECO Chemie, Netherlands) in a three-electrode arrangement with silver/silver chloride (Ag/AgCl) as the reference electrode, platinum foil as the counter electrode and a glassy carbon electrode (GCE, BAS, 3 mm diameter) as the working electrode. The reference electrode was separated from the working solution by an electrolytic bridge filled with 0.1 M TBAHFP/AN solution. The reference electrode potential was calibrated by using ferrocene oxidation process in the same TBAHFP/AN solution. AN containing 0.1 M TBAHFP was used as the supporting electrolyte solution. Argon was used to deaerate the solution and an argon blanket was maintained over the solution during the experiments.

6,13-Bis(methoxycarbonyl)-1,4,8,11-tetraazacyclotetradeca-4,6,11,13-tetraenato(2–)-κ^{4}N^{1,4,8,11}nickel(II) (4Ni). (a) From Ligand 4: Macrocyclic ligand **4** (0.62 g, 0.002 mol) and nickel acetate tetrahydrate (0.55 g, 0.0022 mol) were refluxed in methanol (200 mL) for 1 h. The reaction mixture was cooled down and left in a refrigerator for crystallisation. The resulting orange precipitate was filtered off and recrystallised from a dichloromethane/methanol mixture (1:5, 300 mL). Yield: 0.64 g (88%).

(b) From Complex 3Ni: Complex **3Ni** (0.341 g, 0.001 mol) was dissolved in ethylenediamine (2.5 mL). The mixture was refluxed for 1 h, cooled and diluted with 25 mL of water. The resulting orange precipitate was filtered off and purified by chromatography on neutral alumina (Merck) with chloroform/methanol (99:1) as eluent. The eluate was evaporated to dryness and the residue recrystallised from dichloromethane/methanol (1:5). Yield: 0.275 g (77%); m.p. 284 °C. Slow evaporation of a solution of **4Ni** in dichloromethane/toluene (1:1) gave crystals suitable for X-ray data collection. $C_{14}H_{20}N_4NiO_4$ (365.0): calcd. C 46.1, H 5.0, N 15.3; found C 46.2, H 5.1, N 15.3. ESI MS: *m/z* 365.3 [$C_{14}H_{20}N_4O_4Ni$ + H]$^+$, 387.3 [$C_{14}H_{20}N_4O_4Ni$ + Na]$^+$. ^{1}H NMR (400 MHz, $CDCl_3$): δ = 7.81 (s, 4 H, =CH-N), 3.73 (s, 6 H, CH_3), 3.38 (s, 8 H, N-CH_2) ppm. ^{13}C NMR (100 MHz, $CDCl_3$): δ = 154.9 (=CH-N), 168.2 (O-C=O), 98,2 (-C=), 51.2 (CH_3), 58.7 (N-CH_2) ppm. UV/Vis (methanol): λ_{max} (ε) = 201 nm (25020 M^{-1} cm^{-1}), 229 (30220), 316 (40640), 374 (5310), 497 (275). IR (nujol): $\tilde{\nu}$ = 1677 vs. (C=O), 1598 vs. (C=N), 1539 m (C=C) cm^{-1}.

6,13-Bis(methoxycarbonyl)-1,4,8,11-tetraazacyclotetradeca-4,6,11,13-tetraenato(2–)-κ^{4}N^{1,4,8,11}copper(II) (4Cu): This complex was obtained following the same procedures: (a) from ligand **4** with copper(II) acetate instead of nickel(II) acetate. Yield: 77%; (b) condensation of **3Cu** with ethylenediamine. Yield: 51%, m.p. 295 °C. $C_{14}H_{20}CuN_4O_4$ (369.9): calcd. C 45.5, H 4.9, N 15.2; found C 45.4, H 5.1, N 15.0. ESI MS: *m/z* 370.2 [$C_{14}H_{20}N_4O_4Cu$ + H]$^+$, 392.2 [$C_{14}H_{20}N_4O_4Cu$ + Na]$^+$. UV/Vis (methanol): λ_{max} (ε) = 205 nm (24540 M^{-1} cm^{-1}), 238 (11730), 286 (64380), 318 (20670), 550 (140). IR (nujol): $\tilde{\nu}$ = 1678 vs. (C=O), 1596 vs. (C=N), 1547 m (C=C) cm^{-1}.

6,14-Bis(methoxycarbonyl)-1,4,8,12-tetraazacyclopentadeca-4,6,12,14-tetraenato(2–)-κ^{4}N^{1,4,8,12}nickel(II) (5Ni): Complex **3Ni** (0.341 g, 0.001 mol) was dissolved in 1,3-propylenediamine (2.5 mL). The mixture was refluxed for 2 h, cooled and diluted with 25 mL of water. The resulting red precipitate was filtered off and purified by chromatography on neutral alumina (Merck) with chloroform methanol (99:1) as eluent. The eluate was evaporated to dryness and the residue recrystallised from dichloromethane/methanol (1:5). Yield: 0.370 g (91%); m.p. 231 °C. Crystals of **5Ni** used for X-ray data collection were obtained by slow evaporation of a dichloromethane/toluene solution. $C_{15}H_{20}N_4NiO_4$ (379.1): calcd. C 47.5, H 5.3, N 14.8; found C 47.6, H 5.4, N 14.4. ESI MS: *m/z* 379.3 [$C_{15}H_{20}N_4O_4Ni$ + H]$^+$, 401.2 [$C_{15}H_{20}N_4O_4Ni$ + Na]$^+$. ^{1}H NMR (400 MHz, $CDCl_3$): δ = 7.61 (s, 2 H) and 7.60 (s, 2 H, =CH-N), 3.72 (s, 6 H, CH_3), 3.36 (t, *J* = 6.7 Hz, 4 H, N-CH_2), 3.18 (s, 4 H, N-CH_2), 1.87 (quint, *J* = 6.7 Hz, 2 H, CH_2) ppm. ^{13}C NMR (100 MHz, $CDCl_3$): δ = 154.9 and 157.9 (=CH-N), 168.2 (O-C=O), 97.3 (-C=), 50.7 (CH_3), 58.7 and 58.7 (N-CH_2), 28.0 (CH_2) ppm. UV/Vis (methanol): λ_{max} (ε) = 238 nm (28995 M^{-1} cm^{-1}), 299 (39510), 370 (5230), 539 (170). IR (nujol): $\tilde{\nu}$ = 1674 m (C=O), 1604 vs. (C=N), 1539 m (C=C) cm^{-1}.

6,14-Bis(methoxycarbonyl)-1,4,8,12-tetraazacyclopentadeca-4,6,12,14-tetraenato(2–)-κ^{4}N^{1,4,8,12}copper(II) (5Cu): This complex was obtained from **3Cu** following the same procedure as for **5Ni**. Yield: 33%, m.p. 238 °C. $C_{15}H_{20}CuN_4O_4$·0.5H_2O (392.9): calcd. C 45.9, H 5.4, N 14.3; found C 45.7, H 5.1, N 14.4. ESI MS: *m/z* 384.1 [$C_{15}H_{20}N_4O_4Cu$ + H]$^+$, 406.1 [$C_{15}H_{20}N_4O_4Cu$ + Na]$^+$. UV/Vis (methanol): λ_{max} (ε) = 203 nm (20700 M^{-1} cm^{-1}), 281 (66080), 314 (21250), 510 (12910), 662 (130). IR (nujol): $\tilde{\nu}$ = 1682 m (C=O), 1613 vs. (C=N), 1549 m (C=C) cm^{-1}.

3,11-Bis(methoxycarbonyl)-1,5,9,13-tetraazacyclohexadeca-1,3,9,11-tetraenato(2–)-κ^{4}N^{1,5,9,13}nickel(II) (6Ni): This complex was obtained from **2Ni** and 1,3-propylenediamine following the same procedure as for **5Ni**. Yield: 23%, m.p. 198 °C. $C_{16}H_{22}N_4NiO_4$ (393.1): calcd. C 48.9, H 5.6, N 14.3; found C 49.1, H 5.9, N 14.0. ESI MS: *m/z* 393.2 [$C_{16}H_{22}N_4O_4Ni$ + H]$^+$, 415.3 [$C_{16}H_{22}N_4O_4Ni$ + Na]$^+$. ^{1}H NMR (400 MHz, $CDCl_3$): δ = 7.36 (s, 4 H, =CH-N), 3.72 (s, 6 H, CH_3), 3.36 (t, *J* = 6.4 Hz, 8 H, N-CH_2), 1.84 (quint, *J* = 6.4 Hz, 4 H, CH_2) ppm. ^{13}C NMR (100 MHz, $CDCl_3$): δ = 157.3 (=CH-N), 168.3 (O-C=O), 98.2 (-C=), 50.6 (CH_3), 54.3 (N-CH_2), 27.9 (CH_2) ppm. UV/Vis (methanol): λ_{max} (ε) = 250 nm (21660 M^{-1} cm^{-1}), 295 (33430), 343 (4820), 493 (140). IR (nujol): $\tilde{\nu}$ = 1665 m (C=O), 1605 vs. (C=N), 1532 vs. (C=C) cm^{-1}.

3,11-Bis(methoxycarbonyl)-1,5,9,13-tetraazacyclohexadeca-1,3,9,11-tetraenato(2–)-κ^{4}N^{1,5,9,13}copper(II) (6Cu): This complex was obtained from **2Cu** and 1,3-propylenediamine following the same procedure as for **5Ni**. Yield: 13%, m.p. 227 °C. $C_{16}H_{22}CuN_4O_4$ (397.9): calcd. C 48.3, H 5.6, N 14.1; found C 48.1, H 5.4, N 14.1. ESI MS: *m*/*z* 398.1 $[C_{16}H_{22}N_4O_4Cu + H]^+$, 420.1 $[C_{16}H_{22}N_4O_4Cu + Na]^+$. UV/Vis (methanol): λ_{max} (ε) = 201 nm (21620 $M^{-1}cm^{-1}$), 277 (64355), 318 (16245), 531 (240), 754 (220). IR (nujol): $\tilde{\nu}$ = 1677 m (C=O), 1610 vs. (C=N), 1536 m (C=C) cm^{-1}.

6,14-Bis(methoxycarbonyl)-1,4,8,12-tetraazacyclopentadeca-4,6,12,14-tetraene Di(hydrogen hexafluorophosphate) {5[HPF$_6$]$_2$}: Complex **5Cu** (0.767 g. 0.002 mol) was stirred in an aqueous solution of methanesulfonic acid (9 mL, 0.02 mol) at room temperature. After 24 h, when all starting complex had dissolved, an excess of solid NH_4PF_6 (1 g) was added and the colourless solid that precipitated filtered off, washed with water and dried under reduced pressure. Yield: 0.687 g (56%), m.p. 245 °C. $C_{15}H_{24}N_4O_4{\cdot}2(PF_6){\cdot}H_2O$ (632.3): calcd. C 28.5, H 4.1, N 8.9; found C 28.4, H 4.5, N 8.8. ESI MS: *m*/*z* 162.1 $[C_{15}H_{24}N_4O_4]^{2+}$, 323.2 $[C_{15}H_{24}N_4O_4 - H]^+$. ^{1}H NMR (400 MHz, CD_3CN): δ = 9.54 (br. m, 2 H, N-H), 9.41 (br. m, 2 H, N-H), 7.43 (d, *J* = 15.4 Hz, 2 H, =CH-N), 7.21 (d, *J* = 15.7 Hz, 2 H, =CH-N), 3.92 (s, 6 H, CH_3), 3.40 (br. m, 4 H, N-CH_2), 3.97 (br. s, 4 H, N-CH_2), 2.20 (quint, 2 H, CH_2) ppm. ^{13}C NMR (100 MHz, CD_3CN): δ = 167.0 and 167.8 (=CH-N), 166.3 (O-C=O), 96.7 (-C=), 53.1 CH_3, 50.1 and 51.4 (N-CH_2), 24.9 (CH_2) ppm. UV/Vis (methanol): λ_{max} (ε) = 235 nm (27190 $M^{-1}cm^{-1}$), 303 (26345). IR (nujol): $\tilde{\nu}$ = 3345 vs. and 3255 (O–H and N–H), 1715 m (C=O), 1664 w and 1625 vs. (C=N and C=C), 845 vs. and 560 m (PF_6) cm^{-1}.

3,11-Bis(methoxycarbonyl)-1,5,9,13-tetraazacyclopentadeca-1,3,9,11-tetraene Di(hydrogen hexafluorophosphate) {6[HPF$_6$]$_2$}: This complex was obtained from **6Ni** following the same procedure. Yield: 56%, m.p. 261 °C. $C_{16}H_{26}N_4O_4{\cdot}2(PF_6){\cdot}H_2O$ (646.4): calcd. C 29.7, H 4.4, N 8.7; found C 30.5, H 4.6, N 8.7. ESI MS: *m*/*z* 169.1 $[C_{16}H_{26}N_4O_4]^{2+}$, 337.2 $[C_{16}H_{24}N_4O_4 - H]^+$. ^{1}H NMR (400 MHz, CD_3CN): δ = 9.66 (br. m, 4 H, N-H), 7.85 (d, *J* = 15.0 Hz, 4 H, =CH-N), 4.00 (s, 6 H, CH_3), 3.70 (br. m, 8 H, N-CH_2), 2.17 (quint, 4 H, CH_2) ppm. ^{13}C NMR (100 MHz, CD_3CN): δ = 176.4 (=CH-N), 165.9 (O-C=O), 101.4 (-C=), 52.3 (CH_3), 48.3 (N-CH_2), 30.1 (CH_2) ppm. UV/Vis [methanol/acetonitrile (9:1)]: λ_{max} (ε) = 252 nm (10630 $M^{-1}cm^{-1}$), 289 (17360). IR (nujol): $\tilde{\nu}$ = 3326 vs. and 3240 (O–H and N–H), 1703 m (C=O), 1672 w and 1637 vs. (C=N and C=C), 851 vs. and 558 m (PF_6) cm^{-1}.

(3,13,17,20,24,34,38,41,44,47,50,53-Dodecaazatricyclo[34.6.6.6^{15,22}]-tetrapentaconta-1,14,16,20,22,35,37,41,43,47,49,53-dodecaene-κ^{8}N)-dinickel(II) Hexafluorophosphate (9NiNi): 6,13-Bis(methoxymethylidene)-1,4,8,11-tetraazacyclotetradeca-4,7,11,14-tetraenato(2-)-nickel(II) dihexafluorophosphate[1] (0.625 g, 1 mmol) and 1,9-nonanediamine (0.158 mL, 1 mmol) were separately dissolved in 25 mL of dry acetonitrile and added dropwise to 100 mL of acetonitrile with a peristaltic pump at a rate of 15 mL h^{-1}. The mixture was then left for 3 h at room temperature and partly evaporated. The remaining 20 mL of solution was diluted with 20 mL of water and applied to a silica gel column (Merck 60 silanized, 25 × 2.5 cm). The column was washed with CH_3CN/H_2O (5:4) and eluted with CH_3CN/H_2O (3:2) with addition of NH_4PF_6 (3 g per 100 mL). The first major band was collected and slowly evaporated to give yellow crystals. Yield: 0.277 g (19.2%). $C_{42}H_{68}F_{24}N_{12}Ni_2P_4$ (1438.3): calcd. C 35.1, H 4.8, N 11.7; found C 34.6, H 4.5, N 11.5. IR (nujol): $\tilde{\nu}$ = 1615 v s, 834 v s, 557 s cm^{-1}. MS (ESI, CH_3CN): *m*/*z* 214.1 $[C_{42}H_{68}N_{12}Ni_2]^{4+}$, 285.2 $[C_{42}H_{67}N_{12}Ni_2]^{3+}$, 334.5 $[(C_{42}H_{68}N_{12}Ni_2)^{4+} + PF_6^-]$, 427.2 $[C_{42}H_{66}N_{12}Ni_2]^{2+}$, 573.2 $[(C_{42}H_{68}N_{12}Ni_2)^{4+} + 2PF_6^-]$. ^{1}H NMR ($CD_3CN$, 400 MHz): δ = 1.31 (br. s, 20 H, γ-, δ- and ε-CH_2), 1.62 (br. s, 8 H, β-CH_2), 3.46–3.57 (m, 24 H, α-CH_2 and ring CH_2CH_2), 7.65 (s, 4 H, =CH-N), 7.50, 7.97 (br. s, 2 × 4 H, N=C-H), 8.06 (br. s, 4 H, N-H) ppm. ^{13}C NMR (CD_3CN, 100 MHz): δ = 26.5, 29.5, 29.9, 30.1 (β-, γ-, δ- and ε-CH_2), 51.7 (α-CH_2), 59.5, 60.2 (br., ring CH_2CH_2), 104.1 (ring =C), 155.1 (br.) and 160.7 (br., HC=N, 164.0 (=CH-N) ppm.

(3,13,17,20,24,34,38,41,44,47,50,53-Dodecaazatricyclo[34.6.6.6^{15,22}]-tetrapentaconta-1,14,16,20,22,35,37,41,43,47,49,53-dodecaene-κ^{8}N)-dicopper(II) Hexafluorophosphate (9CuCu): 6,13-Bis(methoxymethylidene)-1,4,8,11-tetraazacyclotetradeca-4,7,11,14-tetraenato(2-)-copper(II) dihexafluorophosphate[1] (0.364 g, 0.58 mmol) and 1,9-nonanediamine (0.092 mg, 0.58 mmol) were dissolved in 50 mL of dry acetonitrile. After six hours of continuous stirring the mixture was evaporated and dissolved in 20 mL of CH_3CN/H_2O (5:4). The mixture was applied to a silica gel 60 silanized column (20 × 2 cm, Merck), washed with CH_3CN/H_2O (5:4) and eluted with CH_3CN/H_2O (6:4) with addition of NH_4PF_6 (3 g per 100 mL). Red crystals were obtained upon slow evaporation of the solvent. Yield: 0.115 g (13.7%). $C_{42}H_{68}Cu_2F_{24}N_{12}P_4$ (1448.0): calcd. C 34.8, H 4.7, N 11.6; found C 34.6, H 4.6, N 11.4. IR (nujol): $\tilde{\nu}$ = 1617 vs, 840 vs, 557 s cm^{-1}. MS (ESI, CH_3CN): *m*/*z* 217.1 $[C_{42}H_{68}N_{12}Cu_2]^{4+}$, 289.2 $[C_{42}H_{67}N_{12}Cu_2]^{3+}$, 337.8 $[(C_{42}H_{68}N_{12}Cu_2)^{4+} + PF_6^-]$, 433.2 $[C_{42}H_{66}N_{12}Cu_2]^{2+}$, 579.2 $[(C_{42}H_{68}N_{12}Cu_2)^{4+} + 2PF_6^-]$.

Single Crystal X-ray Diffraction: Single crystal X-ray measurements of **10Ni**, **4Cu**, **4Ni**, **5Ni**, **6Ni**, **4**, **4[HCl]$_2$** and **6[HPF$_6$]$_2$** were performed on a Kuma KM4CCD κ-axis diffractometer with graphite-monochromated Mo-K_α radiation at 100 K (**4Ni**, **5Ni**, **6Ni**, **4[HCl]$_2$**, **6[HPF$_6$]$_2$**) or at 120 K (**10Ni**, **4Cu**, **4**). The single crystal was positioned at a distance of 65 mm from the KM4CCD camera. A total of 1150 (**6Ni**), 1204 (**10Ni**, **4Cu**, **4Ni**, **5Ni**, **4**, **4**[HCl]$_2$) and 1332 (**6**[HPF$_6$]$_2$) frames were measured at 1.0° (**10Ni**, **4Cu**, **4Ni**, **5Ni**, **6Ni**, **4**, **4**[HCl]$_2$) and at 0.9° (**6**[HPF$_6$]$_2$) intervals with a counting time of 15 s (**4Cu**, **4**), 20 s (**6**[HPF$_6$]$_2$), 22 s (**5Ni**), 25 s (**10Ni**, **4Ni**), and 30 s (**6Ni** and **4**[HCl]$_2$). The data were corrected for Lorentz and polarisation effects, and a numerical absorption correction was applied for **4Cu** and **6Ni**). Data collection, cell refinement and data reduction were carried out with the Kuma Diffraction programs: CrysAlis CCD and CrysAlis RED.[13]

The structures were solved by direct methods[14] and refined using SHELXL.[15] The refinements were based on F^2 for all reflections except those with very negative F^2 values. Weighted *R* factors (*wR*) and all goodness-of-fit (σ) values are based on F^2. Conventional *R* factors are based on *F* with *F* set to zero for negative F^2. The $F_o^2 > 2\sigma(F_o^2)$ criterion was used only for calculating *R* factors and is not relevant to the choice of reflections for the refinement. The *R* factors based on F^2 are about twice as large as those based on *F*. Most of the hydrogen atoms were located from a differential map and refined isotropically. All remaining hydrogen atoms were located in idealised averaged geometrical positions and allowed to ride on the heavy atoms. The disorder of the toluene molecules located at special positions was resolved (**4Ni** and **5Ni**). Some of the atoms of the counterions were refined isotropically (**6[HPF$_6$]$_2$**). Scattering factors were taken from Tables 6.1.1.4 and 4.2.4.2 in ref.[16]

10Ni: $C_{16}H_{26}N_4NiO_4$, *fw* = 397.12; *T* = 120 K; λ = 0.71073 Å; triclinic; space group, $P\bar{1}$; unit cell dimensions: *a* = 4.7792(4), *b* = 9.6841(8), *c* = 10.475(1) Å, α = 64.510(9)°, β = 81.876(8)°, γ = 84.052(7)°; *V* = 432.74(7) Å^3; *Z* = 1; D_{calcd} = 1.524 Mg m^{-3}; absorption coefficient: 1.150 mm^{-1}; *F*(000) = 210; crystal size: 0.61 × 0.18 × 0.11 mm^3; θ range for data collection: 3.80–25.00°; index ranges: $-5 \le h \le 5$, $-11 \le k \le 11$, $-12 \le l \le 12$; reflections

collected: 6458; independent reflections: 1530 (R_{int} = 0.0340); refinement method, full-matrix least-squares on F^2; data/restraints/parameters: 1530/0/171; goodness-of-fit on F^2 = 1.096; final R indices [$I > 2\sigma(I)$]: $R1$ = 0.0201, $wR2$ = 0.0479; R indices (all data): $R1$ = 0.0213, $wR2$ = 0.0485; weight: $1/[\sigma^2(F_o^2) + (0.0258P)^2 + 0.0779P]$ where $P = [\mathrm{Max}(F_o^2, 0) + 2F_c^2]/3$; largest diffraction peak and hole: 0.323 and –0.281 e Å^{-3}.

4Cu: $C_{14}H_{18}CuN_4O_4$, fw = 369.86; T = 120 K; λ = 0.71073 Å; monoclinic; space group, $P2_1/c$; unit cell dimensions: a = 8.220(2), b = 6.322(1), c = 15.546(3) Å, α = 90°, β = 108.41(3)°, γ = 90°; V = 766.5(3) Å^3; Z = 2; D_{calcd} = 1.602 Mg m^{-3}; absorption coefficient: 1.451 mm^{-1}; F(000) = 382; crystal size: 0.53 × 0.11 × 0.11 mm^3; θ range for data collection: 3.51–24.99°; index ranges: $-9 \le h \le 9$, $-7 \le k \le 7$, $-18 \le l \le 18$; reflections collected: 11278; independent reflections: 1351 (R_{int} = 0.0485); absorption correction: numerical; max. and min. transmission: 0.89822 and 0.58548; refinement method, full-matrix least-squares on F^2; data/restraints/parameters: 1351/0/115; goodness-of-fit on F^2 = 1.075; final R indices [$I > 2\sigma(I)$]: $R1$ = 0.0398, $wR2$ = 0.1064; R indices (all data): $R1$ = 0.0454, $wR2$ = 0.1114; weight: $1/[\sigma^2(F_o^2) + (0.0840P)^2 + 0.0107P]$ where $P = [\mathrm{Max}(F_o^2, 0) + 2F_c^2]/3$; largest diffraction peak and hole: 0.923 and –0.528 e Å^{-3}.

4Ni: $C_{21}H_{26}N_4NiO_4$, fw = 457.17; T = 100 K; λ = 0.71073 Å; triclinic; space group, $P\bar{1}$; unit cell dimensions: a = 6.3188(5), b = 7.7913(6), c = 11.1511(9) Å, α = 107.429(7)°, β = 98.737(7)°, γ = 95.131(7)°; V = 512.38(7) Å^3; Z = 1; D_{calcd} = 1.482 Mg m^{-3}; absorption coefficient: 0.983 mm^{-1}; F(000) = 240; crystal size: 0.79 × 0.32 × 0.21 mm^3; θ range for data collection: 3.86–25.00°; index ranges: $-7 \le h \le 7$, $-9 \le k \le 9$, $-13 \le l \le 13$; reflections collected: 7602; independent reflections: 1809 (R_{int} = 0.0456); refinement method, full-matrix least-squares on F^2; data/restraints/parameters: 1809/0/218; goodness-of-fit on F^2 = 1.116; final R indices [$I > 2\sigma(I)$]: $R1$ = 0.0208, $wR2$ = 0.0532; R indices (all data): $R1$ = 0.0214, $wR2$ = 0.0541; extinction coefficient: 0.045(4); weight: $1/[\sigma^2(F_o^2) + (0.0248P)^2 + 0.2216P]$ where $P = [\mathrm{Max}(F_o^2, 0) + 2F_c^2]/3$; largest diffraction peak and hole: 0.318 and –0.251 e Å^{-3}.

5Ni: $C_{22}H_{28}N_4NiO_4$, fw = 471.19; T = 100 K; λ = 0.71073 Å; triclinic; space group, $P\bar{1}$; unit cell dimensions: a = 6.714(1), b = 7.550(1), c = 11.307(2) Å, α = 102.94(1)°, β = 104.11(1)°, γ = 94.03(1)°; V = 537.0(2) Å^3; Z = 1; D_{calcd} = 1.457 Mg m^{-3}; absorption coefficient: 0.940 mm^{-1}; F(000) = 248; crystal size: 0.51 × 0.39 × 0.26 mm^3; θ range for data collection: 3.76–24.99°; index ranges: $-7 \le h \le 7$, $-8 \le k \le 8$, $-13 \le l \le 13$; reflections collected: 7848; independent reflections: 1885 (R_{int} = 0.0867); refinement method, full-matrix least-squares on F^2; data/restraints/parameters: 1885/79/208; goodness-of-fit on F^2 = 1.094; final R indices [$I > 2\sigma(I)$]: $R1$ = 0.0650, $wR2$ = 0.1749; R indices (all data): $R1$ = 0.0685, $wR2$ = 0.1833; weight: $1/[\sigma^2(F_o^2) + (0.1318P)^2 + 0.3394P]$ where $P = [\mathrm{Max}(F_o^2, 0) + 2F_c^2]/3$; largest diffraction peak and hole: 0.869 and –0.804 e Å^{-3}.

6Ni: $C_{16}H_{22}N_4NiO_4$, fw = 393.09; T = 100 K; λ = 0.71073 Å; monoclinic; space group, $P2_1/c$; unit cell dimensions: a = 7.6007(5), b = 7.4494(4), c = 15.3716(9) Å, α = 90°, β = 107.166(5)°, γ = 90°; V = 831.58(9) Å^3; Z = 2; D_{calcd} = 1.570 Mg m^{-3}; absorption coefficient: 1.197 mm^{-1}; F(000) = 412; crystal size: 0.44 × 0.39 × 0.16 mm^3; θ range for data collection: 3.31–24.99°; index ranges: $-9 \le h \le 9$, $-8 \le k \le 8$, $-18 \le l \le 18$; reflections collected: 11670; independent reflections: 1455 (R_{int} = 0.0195); Absorption correction: numerical; max. and min. transmission: 0.82771 and 0.63239; refinement method, full-matrix least-squares on F^2; data/restraints/parameters: 1455/0/160; goodness-of-fit on F^2 = 1.072; final R indices [$I > 2\sigma(I)$]: $R1$ = 0.0207, $wR2$ = 0.0499; R indices (all data): $R1$ = 0.0232, $wR2$ = 0.0510; extinction coefficient: 0.01(2); weight: $1/[\sigma^2(F_o^2) + (0.0261P)^2 + 0.5008P]$ where $P = [\mathrm{Max}(F_o^2, 0) + 2F_c^2]/3$; largest diffraction peak and hole: 0.322 and –0.239 e Å^{-3}.

4: $C_{14}H_{20}N_4O_4$, fw = 308.34; T = 120 K; λ = 0.71073 Å; monoclinic; space group, $P2_1/c$; unit cell dimensions: a = 4.2689(9), b = 19.479(4), c = 9.630(2) Å, α = 90°, β = 109.89(3)°, γ = 90°; V = 753.0(3) Å^3; Z = 2; D_{calcd} = 1.360 Mg m^{-3}; absorption coefficient: 0.101 mm^{-1}; F(000) = 328; crystal size: 0.70 × 0.12 × 0.11 mm^3; θ range for data collection: 3.86–25.00°; index ranges: $-5 \le h \le 5$, $-23 \le k \le 23$, $-11 \le l \le 11$; reflections collected: 11347; independent reflections: 1315 (R_{int} = 0.0807); refinement method, full-matrix least-squares on F^2; data/restraints/parameters: 1315/0/140; goodness-of-fit on F^2 = 1.016; final R indices [$I > 2\sigma(I)$]: $R1$ = 0.0489, $wR2$ = 0.1111; R indices (all data): $R1$ = 0.0776, $wR2$ = 0.1261; weight: $1/[\sigma^2(F_o^2) + (0.0672P)^2]$ where $P = [\mathrm{Max}(F_o^2, 0) + 2F_c^2]/3$; largest diffraction peak and hole: 0.250 and –0.242 e Å^{-3}.

4[HCl]$_2$: $C_{14}H_{26}Cl_2N_4O_6$, fw = 417.29; T = 100 K; λ = 0.71073 Å; triclinic; space group, $P\bar{1}$; unit cell dimensions: a = 7.676(1), b = 8.3605(9), c = 8.545(1) Å, α = 83.504(9)°, β = 71.69(1)°, γ = 68.56(1)°; V = 484.6(1) Å^3; Z = 1; D_{calcd} = 1.430 Mg m^{-3}; absorption coefficient: 0.373 mm^{-1}; F(000) = 220; crystal size = 0.14 × 0.12 × 0.08 mm^3; θ range for data collection: 3.49–24.99°; index ranges: $-9 \le h \le 9$, $-9 \le k \le 9$, $-10 \le l \le 10$; reflections collected: 7509; independent reflections: 1704 (R_{int} = 0.0332); refinement method, full-matrix least-squares on F^2; data/restraints/parameters: 1704/0/170; goodness-of-fit on F^2: 1.002; final R indices [$I > 2\sigma(I)$]: $R1$ = 0.0278, $wR2$ = 0.0593; R indices (all data): $R1$ = 0.0400, $wR2$ = 0.0627; weight: $1/[\sigma^2(F_o^2) + (0.0337P)^2]$ where $P = [\mathrm{Max}(F_o^2, 0) + 2F_c^2]/3$; largest diffraction peak and hole: 0.185 and –0.186 e Å^{-3}.

6[HPF$_6$]$_2$: $C_{16}H_{26}F_{12}N_4O_4P_2$, fw = 628.35; T = 100 K; λ = 0.71073 Å; tetragonal; space group, $I4/m$; unit cell dimensions: a = 19.025(3), b = 19.025(3), c = 27.271(6) Å, α = 90°, β = 90°, γ = 90°; V = 9871(3) Å^3; Z = 16; D_{calcd} = 1.691 Mg m^{-3}; absorption coefficient: 0.299 mm^{-1}; F(000) = 5120; crystal size: 0.56 × 0.28 × 0.28 mm^3; θ range for data collection: 3.38–25.00°; index ranges: $-22 \le h \le 22$, $-22 \le k \le 22$, $-32 \le l \le 32$; reflections collected: 72505; independent reflections: 4439 (R_{int} = 0.0441); refinement method, full-matrix least-squares on F^2; data/restraints/parameters: 4439/133/449; goodness-of-fit on F^2 = 1.108; final R indices [$I > 2\sigma(I)$]: $R1$ = 0.0731, $wR2$ = 0.2067; R indices (all data): $R1$ = 0.0805, $wR2$ = 0.2158; weight: $1/[\sigma^2(F_o^2) + (0.1317P)^2 + 34.2860P]$ where $P = [\mathrm{Max}(F_o^2, 0) + 2F_c^2]/3$; largest diffraction peak and hole: 1.179 and –1.605 e Å^{-3}.

CCDC-606234 to -606241 (for **4**, **4Cu**, **4Ni**, **5Ni**, **6Ni**, **10Ni**, **4[HCl]$_2$** and **6[HPF$_6$]$_2$**, respectively) contain the supplementary crystallographic data for this paper. These data can be obtained free of charge from The Cambridge Crystallographic Data Centre via www.ccdc.cam.ac.uk/data_request/cif.

Acknowledgments

This work was financially supported by the State Committee for Scientific Research (MEiN: project 4 T09A 048 23). The X-ray measurements were undertaken in the Crystallographic Unit of the Physical Chemistry Laboratory at the Chemistry Department of the University of Warsaw. S. D. and K. W. are very grateful to the Polish State Committee for Scientific Research (MEiN) for financial support within the project 3 T09A 018 28 and A. W. within the project 120-501/68-BW-1681/18/05.

[1] B. Korybut-Daszkiewicz, A. Więckowska, R. Bilewicz, S. Domagała, K. Woźniak, *J. Am. Chem. Soc.* **2001**, *123*, 9356–9366.
[2] B. Korybut-Daszkiewicz, A. Więckowska, R. Bilewicz, S. Domagała, K. Woźniak, *Angew. Chem. Int. Ed.* **2004**, *43*, 1700–1704.
[3] a) S. Takamura, T. Yoshimiya, S. Kameyama, A. Nishida, H. Yamamoto, M. Noguchi, *Synthesis* **2000**, 637–664; b) M. Nakane, H. Gollhan, C. R. Hutchinson, P. L. Knutson, *J. Org. Chem.* **1980**, *45*, 2536–2538.
[4] E.-G. Jäger, *Z. Chem.* **1968**, *8*, 392.
[5] D. P. Riley, D. H. Busch, *Inorg. Synth.* **1978**, *18*, 36.
[6] A. Rybka, R. A. Koliński, S. Domagała, J. Kłak, J. Mroziński, K. Woźniak, B. Korybut-Daszkiewicz, *Inorg. Chim. Acta* **2006**, *359*, 4526–4534.
[7] N. Alcock, W.-K. Lin, A. Jircitano, J. D. Mokren, P. V. W. R. Corfield, G. Johnson, G. Novotnak, C. Cairns, D. H. Busch, *Inorg. Chem.* **1987**, *26*, 440–452.
[8] W. Grochala, A. Jagielska, K. Woźniak, A. Więckowska, R. Bilewicz, B. Korybut-Daszkiewicz, J. Bukowska, L. Piela, *J. Phys. Org. Chem.* **2001**, *14*, 63–73.
[9] R. Bilewicz, A. Więckowska, B. Korybut-Daszkiewicz, A. Olszewska, N. Feeder, K. Woźniak, *J. Phys. Chem. B* **2000**, *104*, 11430–11434.
[10] A. Wieckowska, R. Bilewicz, S. Domagala, K. Wozniak, B. Korybut-Daszkiewicz, A. Tomkiewicz, J. Mrozinski, *Inorg. Chem.* **2003**, *42*, 5513–5522.
[11] S. Domagała, A. Więckowska, J. Kowalski, A. Rogowska, J. Szydłowska, B. Korybut-Daszkiewicz, R. Bilewicz, K. Woźniak, *Chem. Eur. J.* **2006**, *12*, 2967–2981.
[12] M. Vincenti, *J. Mass Spectrom.* **1995**, *30*, 925–939.
[13] Oxford Diffraction (**2001**). *CrysAlis CCD* and *CrysAlis RED*. Oxford Diffraction Poland, Wrocław, Poland.
[14] G. M. Sheldrick, *Acta Crystallogr. Sect. A* **1990**, *46*, 467–473.
[15] G. M. Sheldrick, *SHELXL93*. *Program for the Refinement of Crystal Structures*, University of Göttingen, Germany.
[16] *International Tables for Crystallography* (Ed.: A. J. C. Wilson), Kluwer, Dordrecht, **1992**, vol. C.

Received: May 3, 2006
Published Online: November 27, 2006

